ELSEVIER

Journal of Structural Geology 26 (2004) 1137–1156

JOURNAL OF STRUCTURAL GEOLOGY

www.elsevier.com/locate/jsg

Aeromagnetic patterns of half-graben and basin inversion: implications for sediment-hosted massive sulfide Pb–Zn–Ag exploration

P.G. Betts*, D. Giles, G.S. Lister

School of Geosciences, Australian Crustal Research Centre, Monash University, Melbourne, Victoria 3800, Australia

Received 20 January 2003; received in revised form 24 June 2003; accepted 2 July 2003

Abstract

The inverted extensional basins of the Palaeoproterozoic North Australian Craton are amongst the most metallogenically endowed on earth for sediment-hosted massive sulphide (SHMS) Pb–Zn–Ag deposits. Faults that evolved during the evolution of these basins are an important exploration vector as they have behaved as conduits for mineralizing fluids, controlled facies architecture, and impacted on hydrothermal convection cells. We attempt to map out ancient normal faults using integrated structural and aeromagnetic analysis to identify faults that are either buried beneath younger cover or have been inverted during later orogenic events. This technique can be used for targeting potential conduits for mineralising fluids during SHMS Pb–Zn–Ag exploration, as well as a tool to map the architecture of extensional basins. We have constructed simplified cross-sections of half-graben and inverted half-graben and have forward modelled their magnetic response. The aeromagnetic signature of a pre-inverted half-graben shows that the tilt block is characterised by a shallow magnetic gradient related to the shallowing of the magnetic marker beneath the half-graben. Normal offset of the marker unit across a normal fault is characterised by a steeper magnetic gradient, as the depth to the marker horizon increases. Simplified cross-sections of isolated growth anticlines and the hanging wall buttressing show that the general shape of the magnetic profiles are maintained until the half-graben has been completely inverted and the magnetic marker horizon displays reverse offset along the reactivated normal fault.

Keywords: Basin inversion; Exploration; Aeromagnetic analysis; Mount Isa Inlier; Normal fault; Australia

1. Introduction

The relationship between sediment-hosted massive sulfide (SHMS) Pb–Zn–Ag mineralization and faults active during basin development is well-established in many endowed regions such as the North Australian Craton and the Selwyn Basin, Canada (Goodfellow et al., 1993; Etheridge and Wall, 1994; Neudert and McGeough, 1996; Broadbent et al., 1998; Garven et al., 2001; Selley et al., 2001; Betts and Lister, 2002; Nelson et al., 2002; Ord et al., 2002; Betts et al., 2003). The basin fault architecture is important for SHMS Pb–Zn–Ag mineralisation because active faults facilitate transport of metalliferous brines from deep parts of the basin to the surface or near surface (Gustafson and Williams, 1981). The transport of hot basinal fluids from deeper levels of the basin impacts on local geotherms, which directly influences fluid migration cells (Hobbs et al., 2000; Garven et al., 2001). Seismic activity facilitates episodic fluid migration via mechanisms such as fault valve activity (Sibson, 1995) or seismic pumping (Sibson et al., 1975), which may explain the bedded ore facies characteristic of many SHMS Pb–Zn–Ag deposits (e.g. HYC). Rupture of basin faults at the surface influences facies architecture in the successions that host the deposits. Therefore, an understanding of the fault architecture associated with SHMS Pb–Zn–Ag mineralization is a fundamental exploration vector for this deposit type.

Many basins that host SHMS Pb–Zn–Ag deposits are no longer pristine and have been overprinted by intense crustal shortening (e.g. Selwyn Basin, Canada: Goodfellow et al., 1993; Isa Superbasin, North Australian Craton: Southgate et al., 2000a). Reactivation of the basinal faults (commonly normal faults) during basin inversion often obscures the original fault displacement. During extreme crustal shortening, the pre-shortening movement of the fault may be completely obscured, leading to misinterpretations of the timing and significance of the faults. Moreover, sustained basinal fluid flow along deformation-induced fractures (e.g. Cox et al., 2001), where fault permeability is repeatedly

* Corresponding author. Tel.: +61-39905-4150; fax: +61-39905-5062.
E-mail address: pbetts@mail.earth.monash.edu.au (P.G. Betts).

0191-8141/$ - see front matter © 2004 Elsevier Ltd. All rights reserved.
doi:10.1016/j.jsg.2003.11.020

renewed during episodic seismogenic slipping, can occur throughout the extensional and inversion history of the basin. Developing an understanding of basin inversion processes is important for understanding and mapping the basin fault architecture within a mineralized inverted extensional basin.

Our understanding of basin inversion processes and geometry has been enhanced by seismic reflection datasets (Badley et al., 1989; Roberts, 1989; Hill et al., 1995; Lowell, 1995), analogue modelling (McClay, 1989, 1995), and theoretical studies (Hayward and Graham, 1989; Williams et al., 1989). Most studies analyse inversion geometries in cross-section, and often at the scale of a half-graben or basin. In contrast, there are relatively few studies assessing complicated map patterns that form during inversion (e.g. Williams et al., 1989; Kelly et al., 1999; Betts, 2001). Basin inversion studies have generally, but not exclusively, been driven by petroleum exploration (e.g. MacGregor, 1995), where inverted basins display relatively mild to moderate ($<25\%$) crustal shortening. Application of basin inversion studies to the minerals industry is in its infant stages, yet nearly all endowed SHMS Pb–Zn–Ag provinces are the remnants of inverted basins (e.g. Selwyn Basin, Isa Superbasin) (Betts et al., 2003).

In this paper we describe the different styles of basin inversion structures formed during the ca. 1600–1500 Ma Isan Orogeny throughout the Western Fold Belt of the Mount Isa Inlier. This belt displays heterogeneous strain and thus provides inversion examples in areas of different strain intensity. The basin fault architecture is well understood allowing the relationship between basin structures and inversion to be determined. We show map patterns associated with various inversion geometries and processes that provide criteria for identifying inverted structures in poly-deformed terranes. We also model theoretical aeromagnetic responses for various inversion scenarios that provide a means of identifying inversion structures in poorly exposed terranes. These are the datasets that are typically used for minerals exploration. The results shown in this study are applicable in the Western Fold Belt, and provide a generic tool for mapping the structural architecture of any inverted basin, provided the basin is characterised by a relatively simple magnetic stratigraphy, including those of known or potential SHMS Pb–Zn–Ag endowment.

2. Geological setting

The North Australian Craton preserves numerous stacked and unconformity-bound Palaeoproterozoic basins that evolved between ca. 1800 and 1590 Ma (Plumb et al., 1990; Eriksson et al., 1993; Etheridge and Wall, 1994; O'Dea et al., 1997a,b; Andrews, 1998; Betts et al., 1998; Rawlings, 1999; Page et al., 2000; Scott et al., 2000;

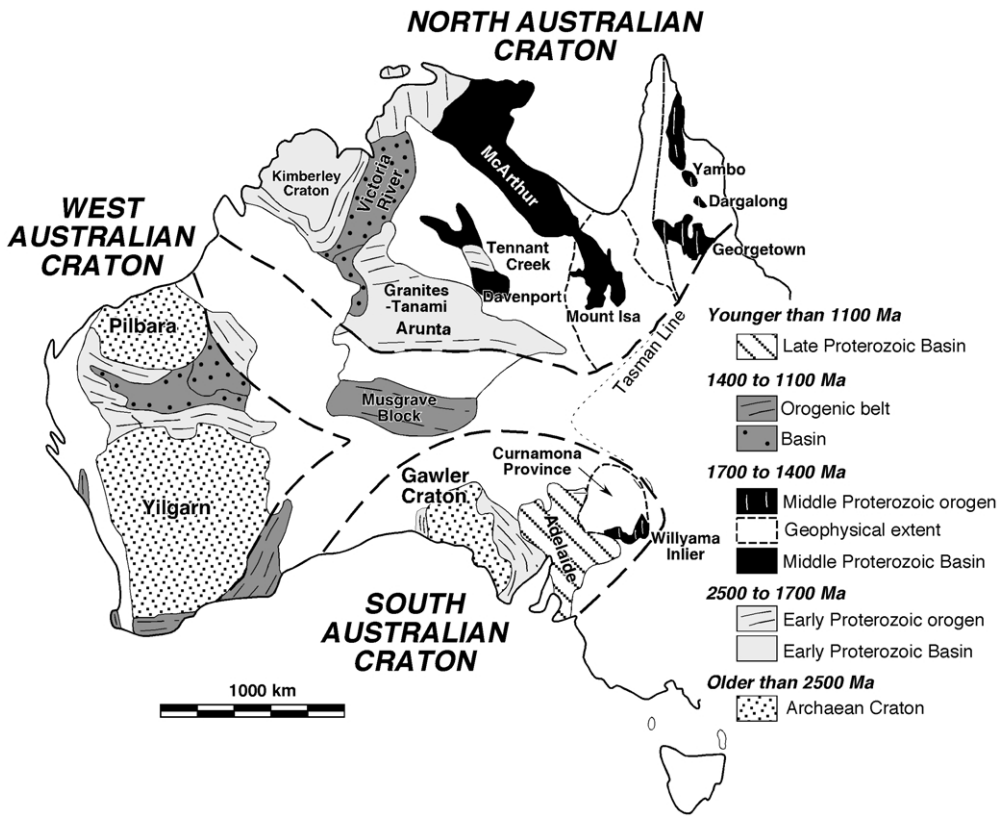

Fig. 1. Simplified geological map of the distribution of the remnants of major basins preserved throughout the North Australian Craton (after Myers et al. (1996)).

Southgate et al., 2000a; Giles et al., 2002). These basins formed in the over-riding plate of a N-dipping subduction system that evolved along the southern margin of the craton (Scott et al., 2000; Giles et al., 2002). The basins are best preserved and understood in the Mount Isa Inlier and McArthur Basin, although contemporary basins evolved in the Davenport Province and the Curnamona Province to the south (Fig. 1). The depositional and thermal evolution of these basins is remarkably coherent across the entire North Australian Craton (Rawlings, 1999; Southgate et al., 2000a; Giles et al., 2002).

In the western Mount Isa Inlier three superbasins have been delineated. These are termed the Leichhardt Superbasin (ca. 1800–1740 Ma), Calvert Superbasin (ca. 1730–1690 Ma) and Isa Superbasin (ca. 1670–1595 Ma; Jackson et al., 2000) (Fig. 2). The Isa Superbasin and equivalent successions in the McArthur Basin contain several large SHMS Pb–Zn–Ag deposits including HYC, Mount Isa, Hilton, Century and several sub-economic occurrences such as Walford Creek, and Lady Loretta (Fig. 3). U–Pb SHRIMP studies (Page et al., 2000) and Pb–Pb isotopic studies (Carr, 1996), indicate major mineralization episodes at ca. 1652 Ma (Mount Isa, Hilton), ca. 1647 Ma (Lady Loretta), ca. 1640 Ma (HYC, Walford Creek), and ca. 1575 Ma (Century), and imply that, with the exception of Century, the deposits formed at a similar time to the deposition of their host sediments (McGoldrick and Large, 1998).

Several structural and sedimentological field studies in the Western Fold Belt have identified faults that were active during the basin history (e.g. Derrick, 1982, 1996; Etheridge and Wall, 1994; O'Dea and Lister, 1995; O'Dea et al., 1997b; Andrews, 1998; Betts et al., 1998, 1999; Scott et al., 1998; Lister et al., 1999; Betts, 2001). These faults preserve displacement, which is the sum of movements associated with crustal extension and crustal shortening. Therefore, criteria other than displacement are necessary to identify ancient normal faults. Stratal growth towards faults is one of the more reliable of these criteria. Stratal growth has been recognised at the basin-scale (e.g. Bain et al., 1992; O'Dea et al., 1997b), at a local-scale (Andrews, 1998; Betts et al., 1999) and has been interpreted from regional seismic reflection data (Scott et al., 1998). Basin faults are characterized by stratal thickness and variations between the hanging wall and footwall (Derrick, 1982; Nijman et al., 1992; Andrews, 1998; Betts et al., 1998, 1999; Lister et al., 1999) as well as deposition of additional stratigraphic packages across faults (Betts, 2001). O'Dea et al. (1997b) and Betts et al. (1999) also used amalgamated syn-rift unconformities to identify regions of local uplift and depositional hiatus, and interpreted these as possible remnant tilt-block crests.

Sedimentation and volcanism during the development of the Leichhardt Superbasin was controlled by half-graben bounding normal faults along the edges of the Leichhardt Rift (Bain et al., 1992; O'Dea et al., 1997b). The polarity of

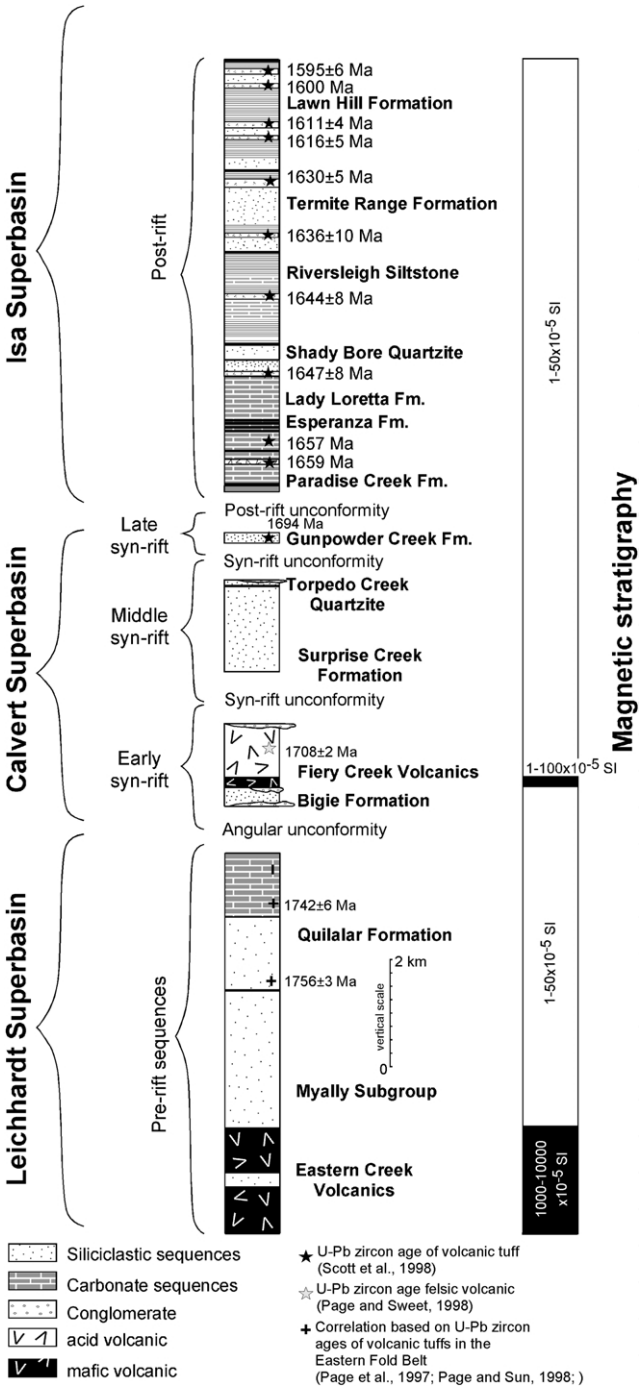

Fig. 2. (a) Simplified lithostratigraphic column of the Western Fold Belt in the Mount Isa Inlier (geochronology data after Scott et al. (1998), Page and Sun (1998), Page and Sweet (1998) and Page et al. (1997)). (b) Magnetic stratigraphic column showing the magnetic susceptibility values of the rock packages (data after Betts (1997)).

half-graben switched along the axis of the rift (O'Dea et al., 1997b). E–W cross-rift structures accommodated the polarity switches and controlled local stratal geometry (O'Dea et al., 1997b). Calvert Superbasin (Mount Isa Rift Event: MIRE) sedimentation was focussed above the Leichhardt Rift. Sedimentation was accompanied by reactivation of the underlying N–S rift-bounding faults

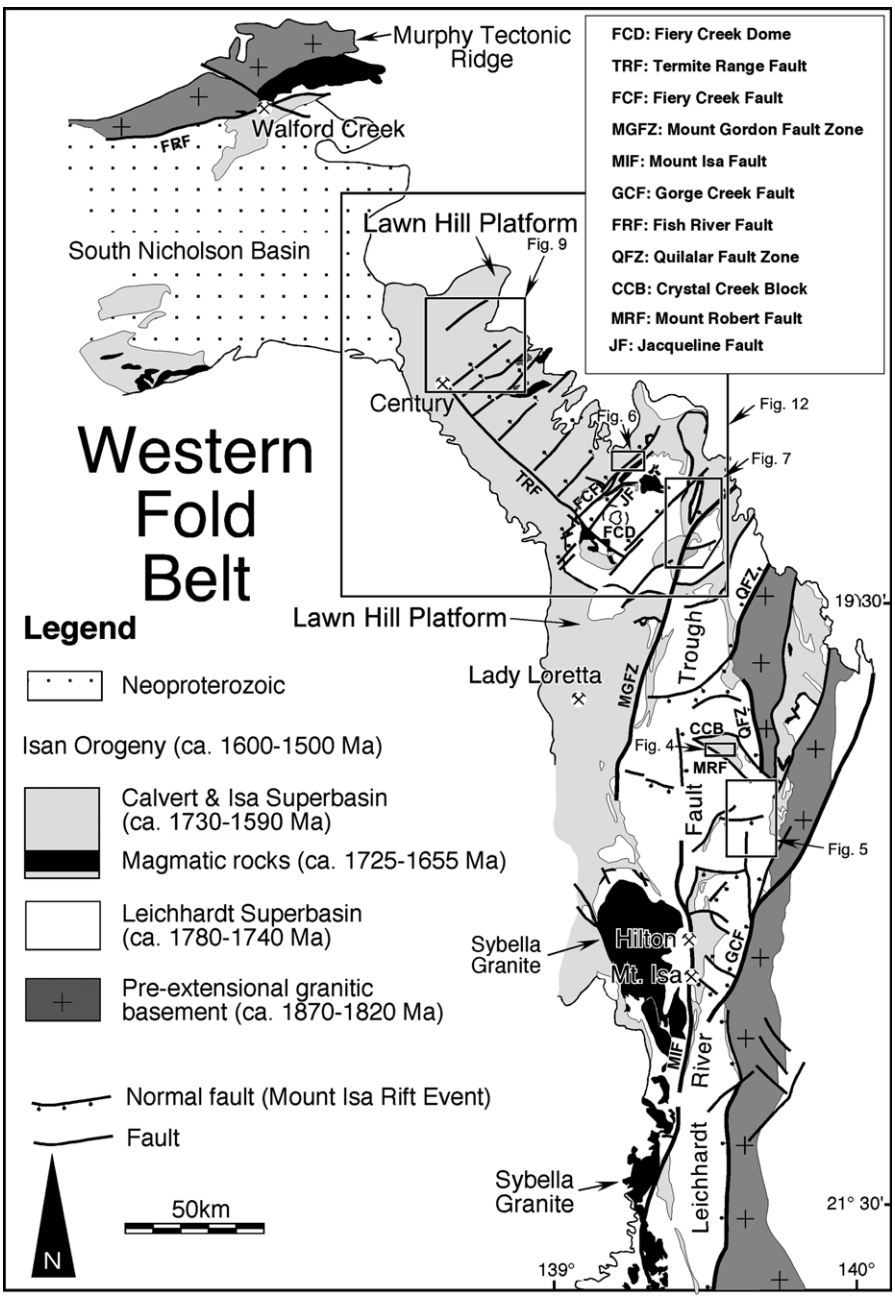

Fig. 3. Simplified geological map of the Western Fold Belt, Mount Isa Inlier showing the distribution of the superbasins and the major elements of the basin architecture (after Betts et al. (1998)). Locations of Figs. 4–7, 9 and 12 are shown.

and E–W cross-rift faults (O'Dea et al., 1997b). These faults controlled the stratal architecture and facies variations (Nijman et al., 1992; Southgate et al., 2000b). Northeast-striking, half-graben bounding normal faults were active in the Lawn Hill Platform (Fig. 3) (Betts et al., 1999; Scott et al., 2000; Betts, 2001). These faults display marked thickness variations and influenced the local facies architecture. Corridors of half-graben are bounded by NW-striking transverse faults (e.g. Termite Range Fault; Fig. 3) (Betts et al., 1999), which facilitated differential normal movement during the MIRE (Betts and Lister, 2001). Scott et al. (1998) interpreted the Termite Range Fault to be an active normal fault during deposition of the Isa Superbasin. This interpretation is supported by stratal thickness variation in the McNamara Group (Andrews, 1998), and suggests a change in the role of the NW- and NE-oriented faults as the basins evolved.

Two episodes of inversion are recognised within the basins. The first inversion was a transient event that occurred between the Leichhardt and Calvert superbasins and resulted in uplift. This resulted in a sedimentary hiatus and erosion in the McArthur Basin (Bull and Rogers, 1996) and gentle folding in the Western Fold Belt (Betts, 1999). Basin development in the North Australian Craton

was terminated by the Isan Orogeny (ca. 1590–1500 Ma) (Bell, 1983; Blake, 1987; O'Dea et al., 1997a). It has been interpreted that the earliest inversion structures formed during an approximate N–S shortening event, followed by inversion during approximate E–W shortening (Bell, 1983; O'Dea et al., 1997a; Lister et al., 1999). Strain associated with the Isan Orogeny is less intense in the Western Fold Belt compared with the central and eastern Mount Isa Inlier. Strain is often focussed by the underlying basin fault architecture (O'Dea and Lister, 1995; Lister et al., 1999; Betts, 2001). Deformation is characterized by upright folding, reactivation of the basin fault architecture and late wrenching (Lister et al., 1999). Strain decreases in the Lawn Hill Platform where line-length balancing restorations suggest less than 25% crustal shortening (Betts et al., 1999).

3. Inversion structures: Western Fold Belt examples

A variety of inversion structures formed in the Western Fold Belt during the Isan Orogeny. This variability is related to the pre-existing fault template, variations in the crustal depth of inversion, multiple stages of deformation, each with different shortening directions, and the decrease in the intensity of crustal shortening to the north. Inversion can occur by either strike-slip reactivation (Lister et al., 1999) or the development of new faults with favourable orientation (Betts, 2001). However, buttressing (O'Dea and Lister, 1995; Lister et al., 1999; Betts, 2001) and the development of isolated growth anticlines above inverted half-graben (O'Dea and Lister, 1995; Betts and Lister, 2002) are the most common inversion structures.

3.1. Hanging wall buttressing

Hanging wall buttressing is a common characteristic of inverted normal faults in the Western Fold Belt (O'Dea and Lister, 1995; O'Dea, 1996; Lister et al., 1999; Betts, 2001) and in other inverted basins (e.g. Western European Alps; Butler, 1989). The expression of buttressing is variable and

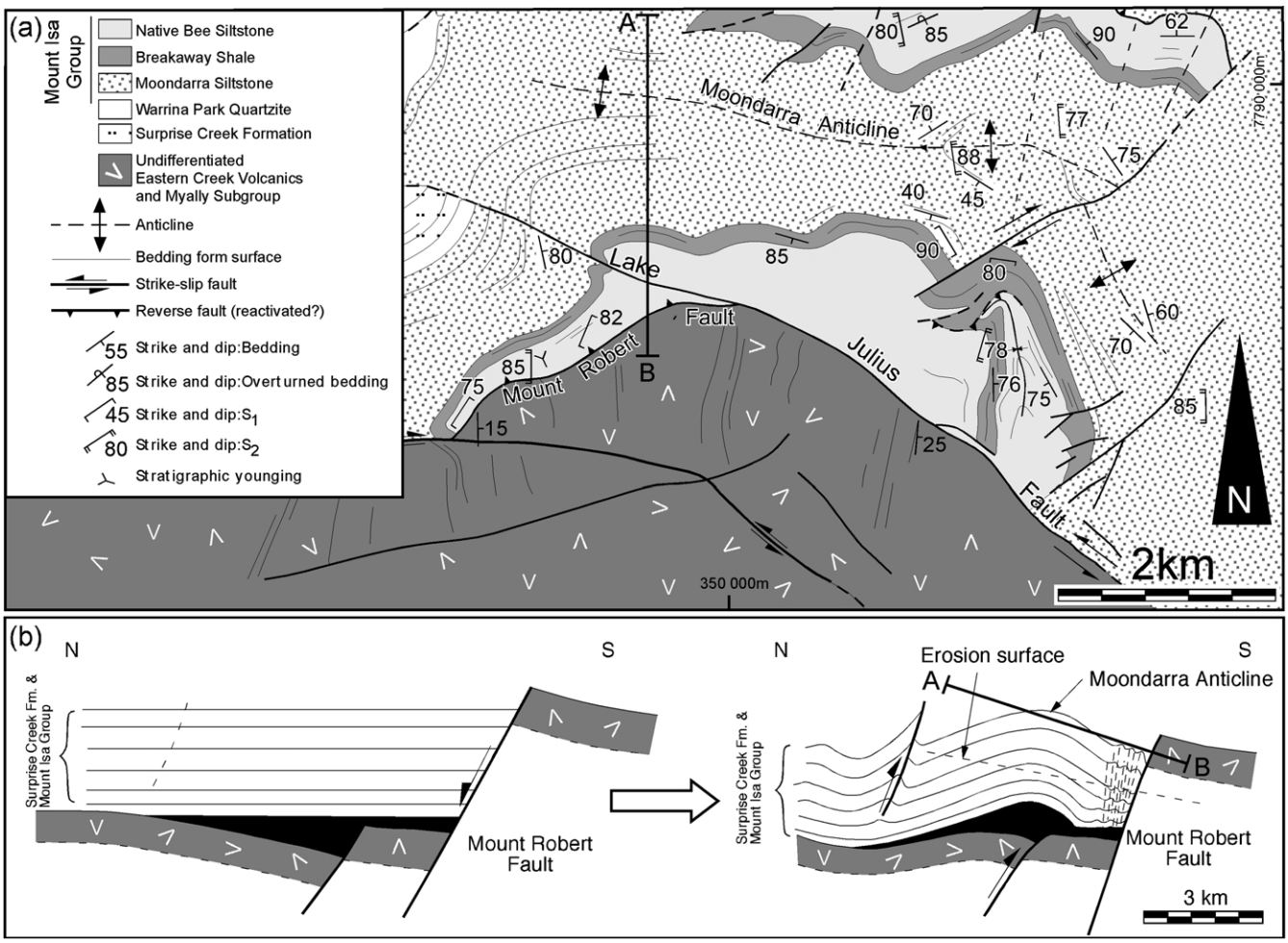

Fig. 4. (a) Structural map of the southern Crystal Creek Block showing buttressing structures developed in the hanging wall of the Mount Robert Fault system (after O'Dea and Lister (1995)). (Location of the map is shown in Fig. 3). (b) Simplified cross-sections showing the reconstructed geometry of the southern Crystal Creek Block and the present day geometry of the Crystal Creek Block illustrating the effects of buttressing and inversion of a buried half-graben (after O'Dea and Lister (1995)).

includes increased intensity of folding proximal to the fault, localized development of slaty cleavage, and enigmatic strain patterns not predicted by the inferred regional shortening direction. The intensity of strain is related to a combination of factors, including the original dip of the basin fault, the intensity of crustal shortening, and the rheology contrasts between the hanging wall and footwall lithologies. Hanging wall buttressing is useful for

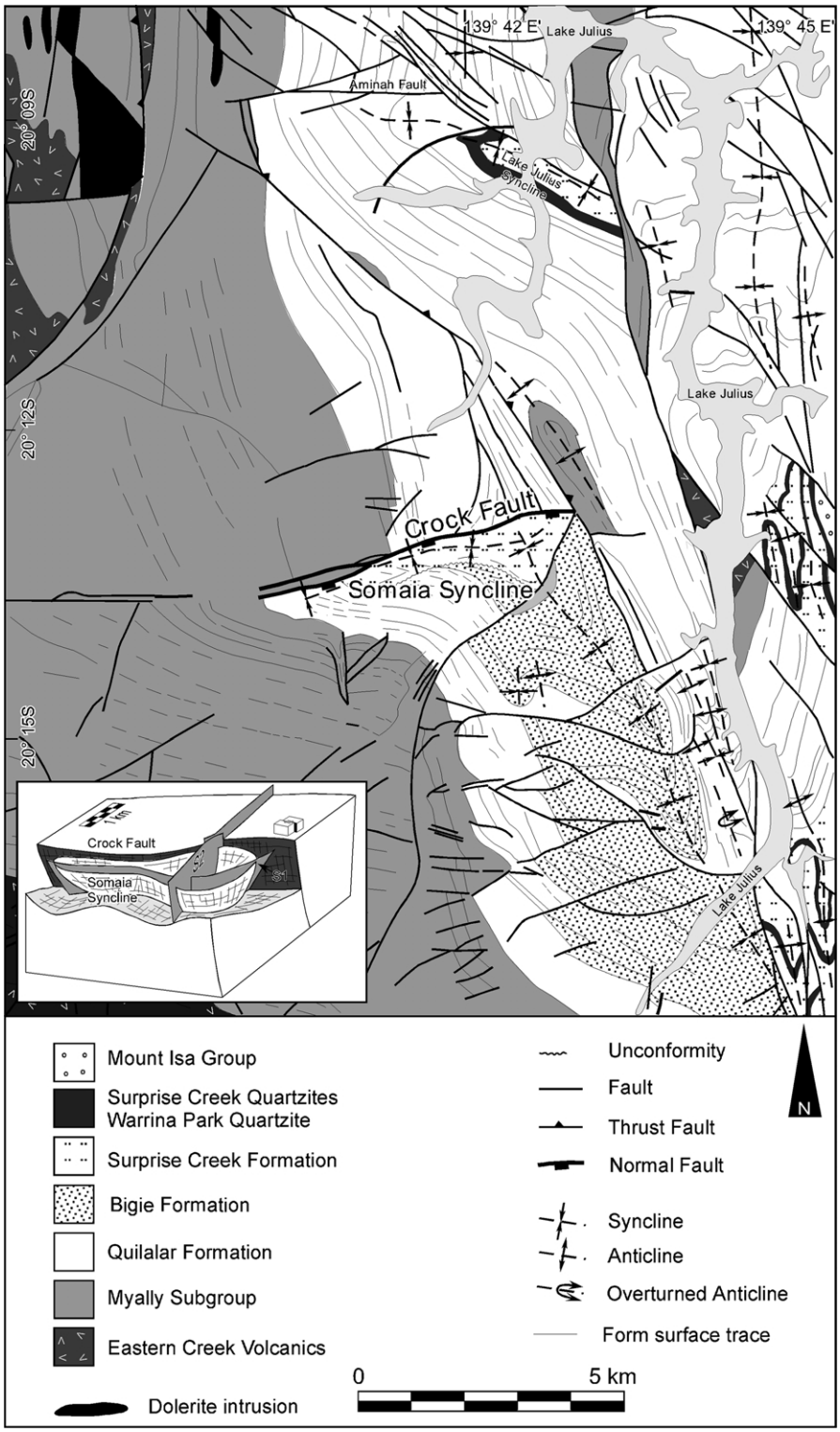

Fig. 5. Geological map of the Somaia Synform showing buttressing against footwall of the south-dipping Crock Fault (after Lister et al. (1999)) (Location of the map is shown in Fig. 3). Inset shows three-dimensional block cartoon of the Somaia Syncline (adapted after Lister et al. (1999)).

identifying inverted normal faults but is not unequivocal as this style of deformation can also occur in the hanging wall of a thrust ramp (Butler, 1989).

Hanging wall buttressing has locally been interpreted in several locations throughout the Western Fold Belt. The influence of rheological contrasts across a normal fault during inversion was demonstrated along the southern Crystal Creek Block in the central Leichhardt River Fault Trough (O'Dea and Lister, 1995) (Figs. 3 and 4). The Mount Robert Fault Zone (Fig. 4) bounds the southern edge of the Crystal Creek Block and separates footwall basaltic and clastic successions of the Leichhardt Superbasin to the south

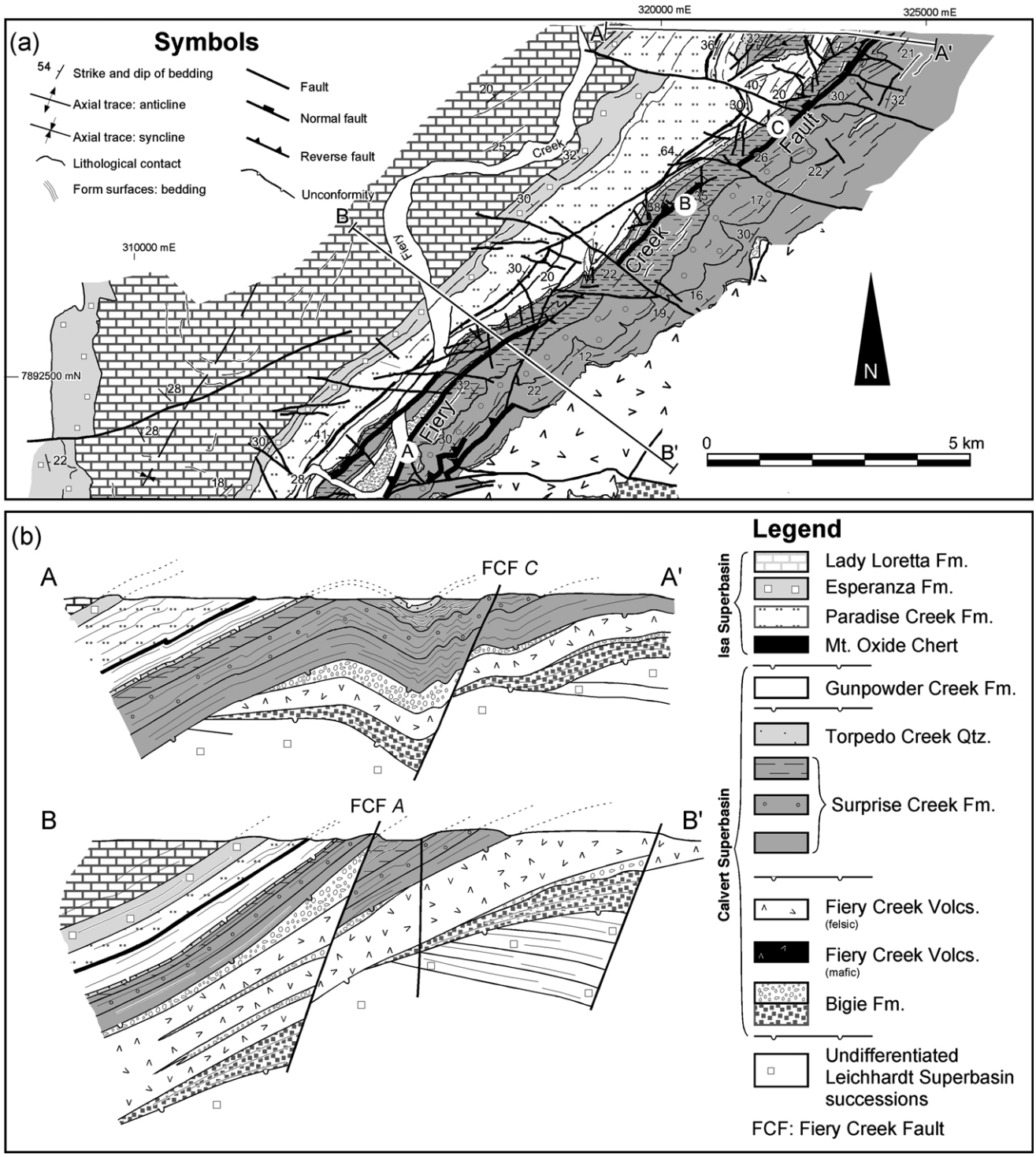

Fig. 6. (a) Map of the deformation compartments that formed in the hanging wall of the Fiery Creek Fault during the basin inversion (after Betts (2001)) (location of the map shown in Fig. 3). (b) Cross-sections across the Fiery Creek Fault system showing differences in the hanging wall geometry produced during inversion (after Betts (2001)).

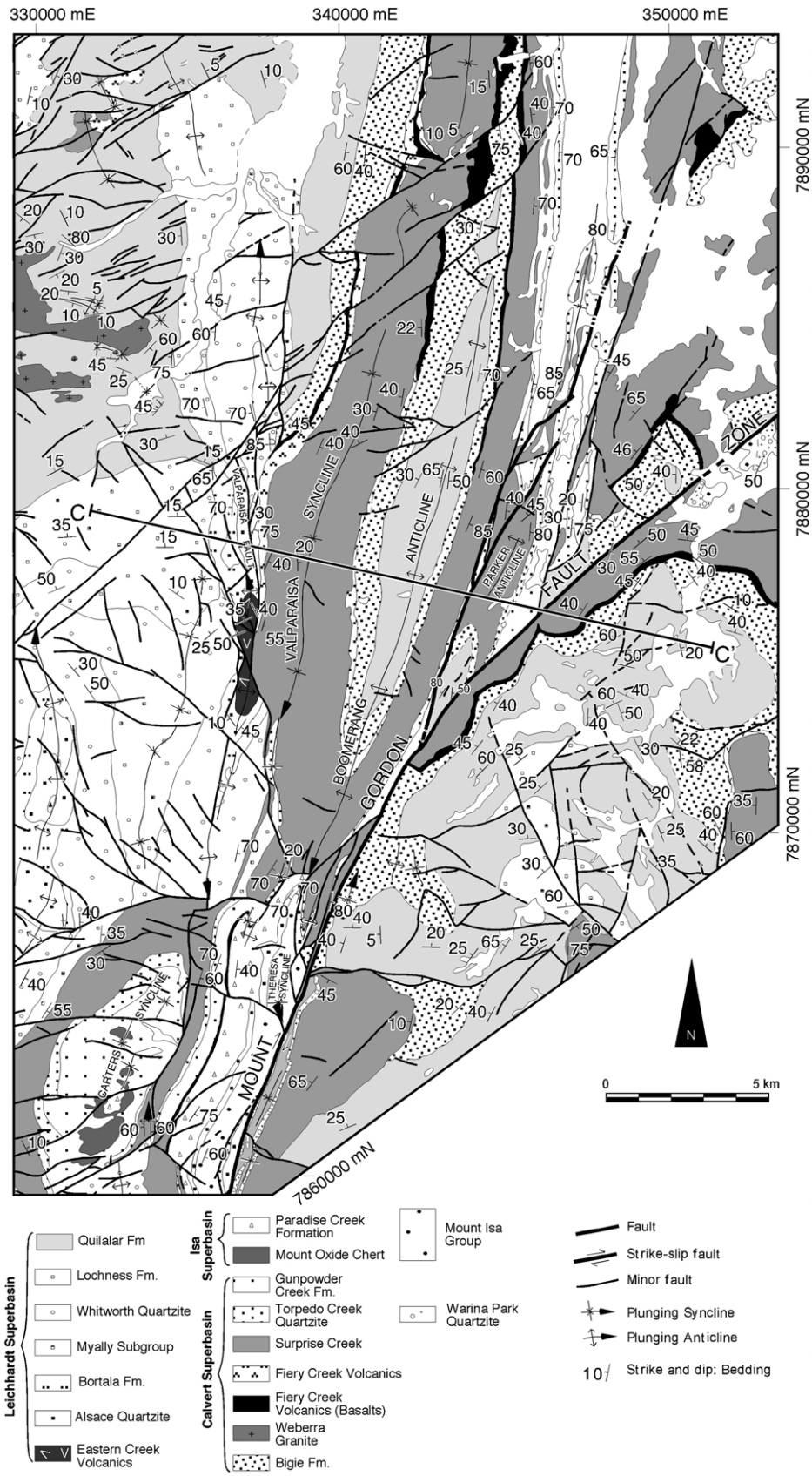

Fig. 7. Map of the Valparaisa Syncline and Boomerang Anticline showing the deformation pattern in the hanging wall of the Mount Gordon Fault Zone (after Derrick et al. (1983)). Location of the map shown in Fig. 3.

from hanging wall sandstone, siltstone, and shale successions of the Calvert and Isa Superbasins to the north (Surprise Creek Formation and Mount Isa Group; Fig. 2). Inversion of the Mount Robert Fault during the Isan Orogeny resulted in the development of localized high strain zones in which a steeply-dipping, fault parallel, slaty cleavage and intense folds developed in the immediate hanging wall of the eastern segment of the Mount Robert Fault. The slaty cleavage is oriented at a small angle to the limbs of tight E–W-trending folds, interpreted to indicate late development in the folding history and a switch from flexural slip folding to flattening (O'Dea and Lister, 1995). Cleavage intensity increases towards the fault zone and locally, a coplanar composite spaced cleavage, axial planar to folds, has overprinted the slaty cleavage suggesting co-axial deformation (O'Dea and Lister, 1995). During this inversion the competent footwall lithologies behaved as stress guides (O'Dea and Lister, 1995). Lister et al. (1999) proposed buttressing for the development of the Somaia Synform in the Lake Julius area (Figs. 3 and 5). The synform is developed in the hanging wall of the S-dipping Crock Fault, which is interpreted as a cross-rift fault during the MIRE (Lister et al., 1999). The synform is interpreted as a MIRE-aged drag syncline (O'Dea, 1996) that was tightened during regional Isan-shortening as the footwall of the Crock Fault behaved as a buttress (Lister et al., 1999).

In the southern Lawn Hill Platform, regional shortening is less intense and normal faults are recognizable (Betts et al., 1999; Betts, 2001); however, the effects of inversion related buttressing are still evident. For example, along the inverted NE-striking Fiery Creek Fault system (Fig. 3) the hanging wall deformation is compartmentalized within discrete blocks separated by ~NW-striking transverse faults (Betts, 2001). Several of the blocks display strain intensification, changes in structural orientation towards parallelism with the fault system, and variation in fold style and intensity with proximity to the fault system. Competency contrasts between rocks in the footwall and hanging wall appear to have controlled the buttressing along the fault system. Buttressing occurs when relatively incompetent rocks in the hanging wall are juxtaposed against relatively competent rocks in the footwall. The greater competency contrasts the more intense hanging wall deformation, which is characterized by increased tightness of macro- and meso-scale folds adjacent to fault segments (Betts, 2001). The folds are often non-cylindrical and characterized by strongly curved axial surfaces (Betts, 2001). Where there are no competency contrasts across the fault there are fewer folds developed in the hanging wall (Fig. 6b). In this situation inversion appears to have been accommodated via fault reactivation and the formation of new reverse faults with shallower dips (e.g. break-back thrusts) (Betts, 2001).

Buttressing along the Fiery Creek Fault system is more common in the segments that were active late in the extensional history of the Calvert Superbasin. Faults active during the earlier stages of the basin history display the most reverse reactivation. Buttressing may have been controlled by the original geometry of the extensional fault. During episodic normal fault development, older normal faults will rotate into shallower orientations, and are therefore into a mechanically and kinematically favourable orientation for reactivation during inversion (Etheridge, 1986; McClay, 1989; Kelly et al., 1999). Younger and steeper normal faults

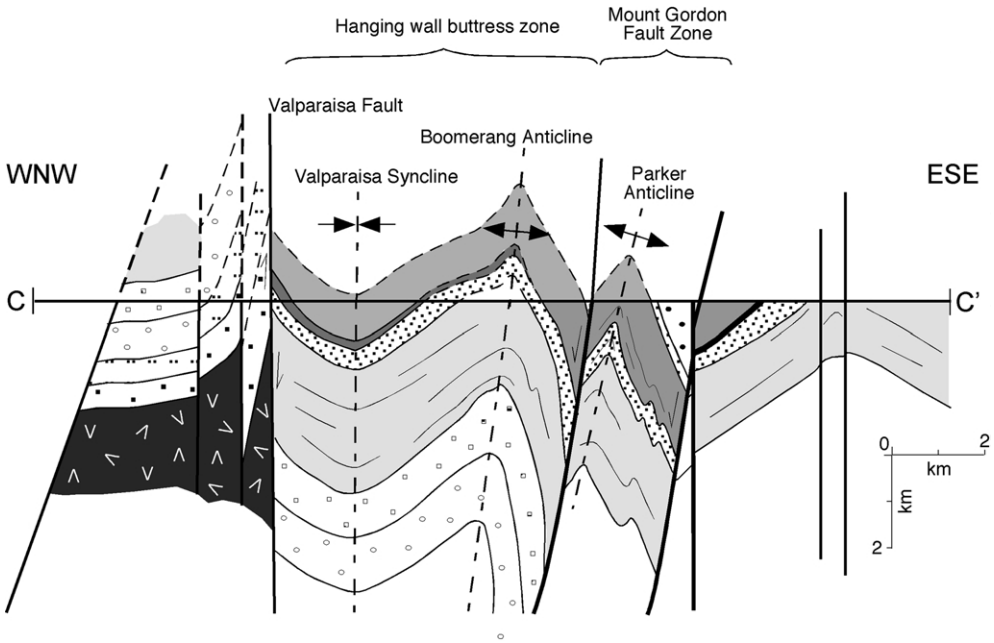

Fig. 8. Cross-section across the Mount Gordon Fault Zone showing variation in deformation pattern between the hanging wall and footwall (location of cross-section is shown in Fig. 7)

have orientations that inhibit reactivation and inversion is accommodated by buttressing (Betts, 2001).

The N- to NE-striking Mount Gordon Fault Zone forms the NW-edge of the Leichhardt River Fault Fault Trough (Fig. 3). It is part of a larger fault system that connects with the Mount Isa Fault system to the south (Fig. 3). The Mount Gordon Fault Zone is steeply dipping and it is interpreted as a regional transcurrent fault that preserves a large component of strike-slip movement (Blake and Stewart, 1992). At its northern extreme the fault splays into several segments that strike to the north and northeast (Fig. 7).

The region to the east of the Mount Gordon Fault Zone is dominated mainly by sedimentary successions of the Leichhardt Superbasin (Myally Subgroup, Quilalar Formtaion), and the lower parts of the Calvert Superbasin (Bigie Formation, and Fiery Creek Volcanics, and Surprise Creek Formation) (Figs. 2 and 7). This region is interpreted to represent a palaeogeographical high during the evolution of the Calvert Superbasin (Derrick, 1982; O'Dea et al., 1997b). The doubly plunging Valparaisa Syncline and Boomerang Anticline lie to the NW of the Mount Gordon Fault Zone. These folds are developed within 5 km of the fault; they are cored by the Quilalar Formation and clastic sediments and volcanic rocks (Bigie Formation, Fiery Creek Volcanics, and Surprise Creek Formation) of the Calvert Superbasin. These folds are close to tight compared with open folds developed in the footwall and in the distal parts of the hanging wall (~10 km) (Figs. 7 and 8). This is interpreted to indicate a zone of increased strain within successions of the Leichhardt and Calvert Superbasins in the proximal hanging wall of the Mount Gordon Fault Zone (Fig. 8). Strain intensification in the hanging wall of the Mount Gordon Fault Zone may indicate that the fault originated as a normal fault during the development of the Calvert and Isa Superbasins. During the second-phase of basin inversion (E–W shortening of the Isan Orogeny), the

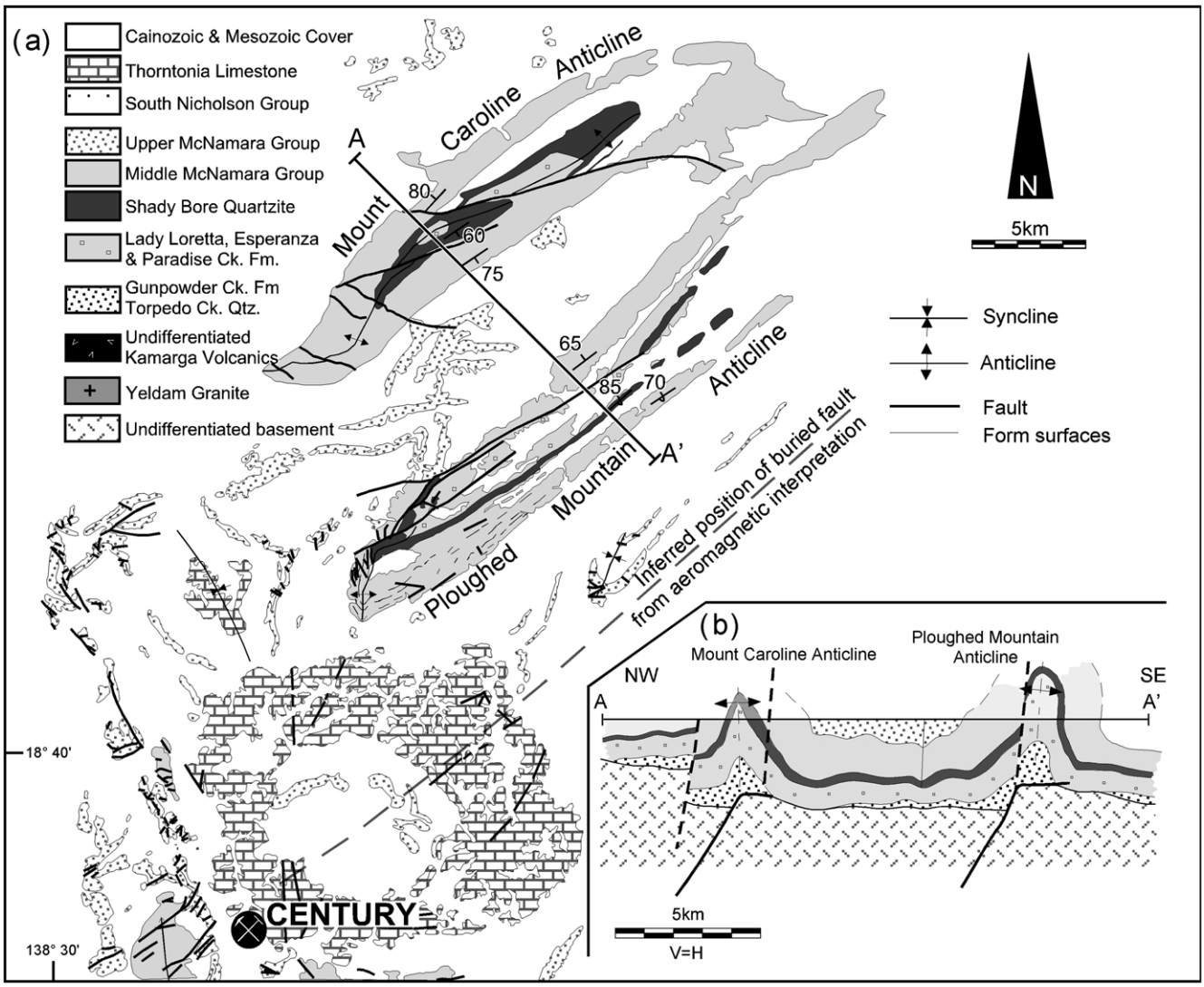

Fig. 9. (a) Map and (b) cross-section across the Ploughed Mountain and Mount Caroline anticlines (after Betts and Lister (2002)). Dashed lines in the cross-section represent late orogenic oblique slip faults that overprint the anticlines. Location of the map is shown in Fig. 3.

competent greenstone and quartz-rich clastic successions may have behaved as a buttress, resulting in intense folding of the syn-rift successions in the proximal hanging wall.

3.2. Isolated growth anticlines

The Ploughed Mountain and Mount Caroline anticlines are two regional-scale folds in the northern part of the exposed Lawn Hill Platform (Fig. 9a). These anticlines are upright and doubly plunging and have axial traces that trend to the NE (Fig. 9a). This orientation is inconsistent with both the N–S and E–W shortening directions inferred for the Isan Orogeny (Bell, 1983; O'Dea et al., 1997a); however, it is parallel to normal faults throughout the Lawn Hill Platform (Betts et al., 1999; Betts and Lister, 2002). This strain is relatively high compared with the rest of the Lawn Hill Platform (e.g. Betts et al., 1999). The amplitudes of the folds are in excess of 3 km; they have inter-limb angles of less than 40° and locally the SE-limbs of the folds are overturned. Betts and Lister (2002) proposed that the Mount Caroline and Ploughed Mountain anticlines were 'isolated anticlines' without a syncline pair, which developed when syn- and post-rift successions were expelled from half-grabens during reverse reactivation of the bounding normal faults (Fig. 9b). The anticlines are overprinted late dextral oblique-slip faults that may be related to either E–W shortening or late orogenic wrenching (Lister et al., 1999). The orientation of the extensional fault architecture active during the MIRE is interpreted as the primarily influence on the anticline geometry and the relatively high strain is interpreted to be related to buttressing against a relatively steep normal fault prior to complete inversion. As shortening continued, folding ceased and new steep dextral oblique-slip faults accommodated inversion.

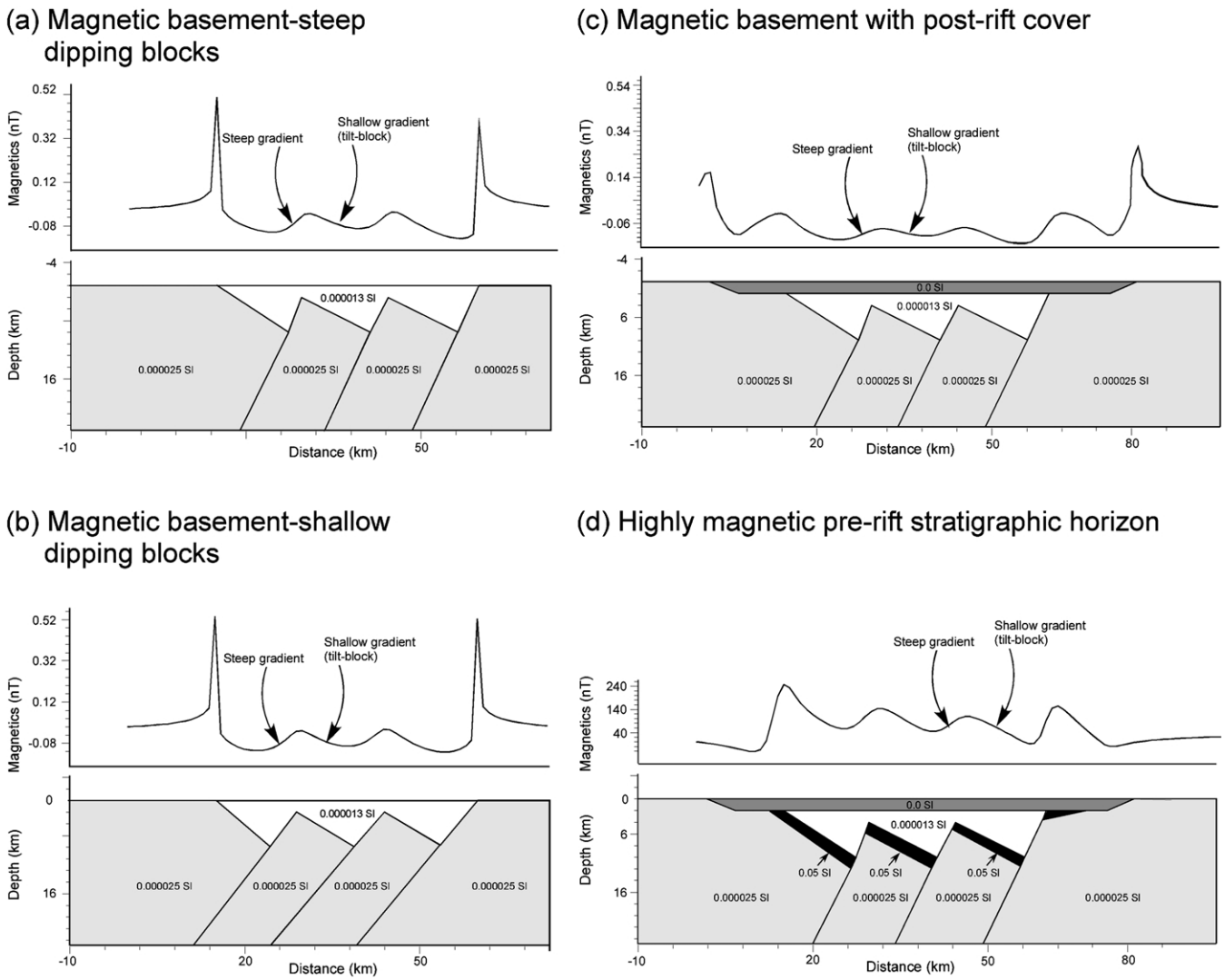

Fig. 10. Theoretical magnetic response of the half-graben. (a) Half-graben with relatively steep normal fault. (b) Half-graben with relatively shallow normal fault. (c) Thin non-magnetic package of post-rift units overlying half-graben. (d) Magnetic marker horizon at the floor of the half-graben that are offset by normal faults.

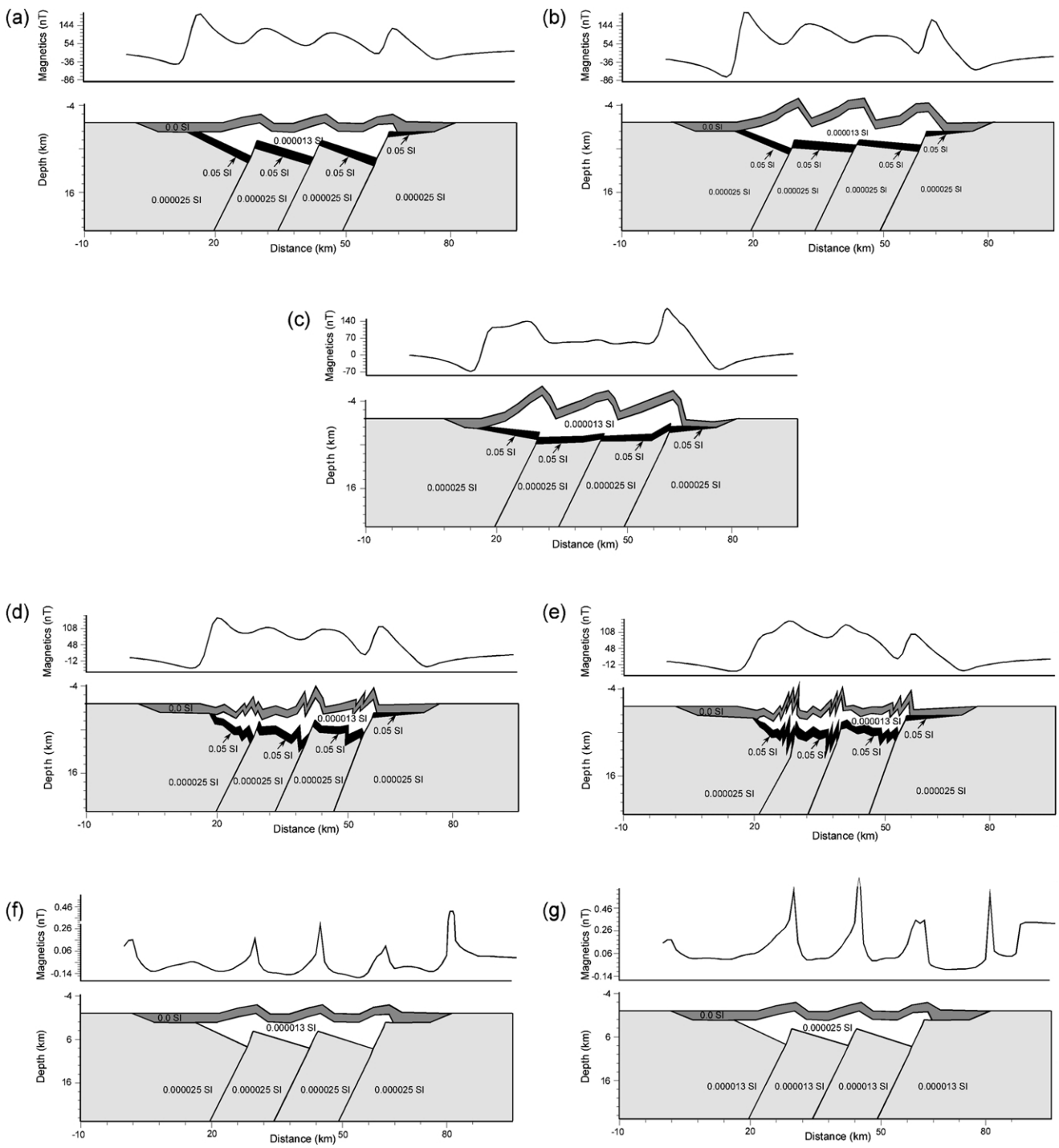

Fig. 11. Theoretical magnetic response of basin inversion structures. (a) Development of growth anticlines with magnetic basement preserving large component of normal offset. (b) Increased inversion with the magnetic basement showing a smaller component of normal offset. (c) Complete inversion with the magnetic basement having reverse reactivation. (d) Relatively mild buttressing during basin inversion resulting in the development of folds in the hanging wall of the normal fault. (e) Intense buttressing with the development of high strain zones in the hanging wall of the normal fault. (f) Mild inversion and development of growth anticline without the magnetic marker horizon in the basement. (g) Mild inversion and development of growth anticline without the magnetic marker horizon in the basement and with magnetic syn-rift fill and weakly magnetized basement. It should be noted that the magnetic response in (f) and (g) may also be produced by folds with similar amplitudes and wavelengths as the half-graben dimensions.

4. Aeromagnetic response of inversion structures

In this section we present numerous aeromagnetic forward models of simplified theoretical cross-sections of half-graben and inverted half-graben geometries (Figs. 10 and 11). The purpose of presenting the models is to illustrate the magnetic patterns produced by these half-graben and inverted half-graben to provide a template to aid in the

recognition of these structures in aeromagnetic data. This approach may be useful for understanding the architecture of buried extensional basins as well as targeting potential conduits for mineralising fluids. The modelled cross-sections show how the magnetic signature changes with the half-graben geometry as well as with increased buttressing and fault reactivation.

Aeromagnetic data show the distribution of magnetic minerals (mainly magnetite) in the Earth's crust (Grant, 1984a,b). Aeromagnetic analysis is a technique that can be used to understand three-dimensional geometry of rocks and overprinting relationships. An advantage of using aeromagnetic data for structural analysis is that it enables recognition of the subsurface geometry of fault offsets of magnetic units (Whiting, 1986; Valenta et al., 1992; Gunn et al., 1997). In addition it allows mapping at large-scales that would be time consuming with conventional field mapping.

There are, however, limitations in using aeromagnetic data for structural analysis. It is difficult to glean information from non-magnetic rock packages. In addition, interpretation and modelling of magnetic data is ambiguous as no single magnetic anomaly has a unique solution (Whiting, 1986; Valenta et al., 1992; Jessell et al., 1993; Gunn et al., 1997; Hornby et al., 1999). No particular structural or geological feature has a unique diagnostic magnetic response; however, it may be possible to recognise patterns in the geophysical response that characterize particular geological structures. These patterns can be recognised by undertaking forward modelling of geophysical data constrained by available geological information. The magnetic data are presented as a 'reduced to the pole' dataset, which removes the effects of the inclination and declination of the Earth's magnetic field. The geometry of the cross-section and the magnetic susceptibility of rock packages are therefore the only influence on the magnetic response.

4.1. Aeromagnetic response of half-graben

The geophysical responses of four theoretical half-graben are presented in Fig. 10. We have used the potential field forward modelling software GM-SYS (Lillie, 1998) to construct the cross-sections and to calculate their magnetic response. In these simplistic models the calculated magnetic profile shows a distinctive response. Fig. 10a and b are simplified cross-sections of weakly magnetic half-graben with a magnetic basement. The shape of the magnetic profile is dependent on the dip of the fault, displacement of the magnetic basement along the fault, the dip of the tilt-block, the spacing between normal faults, and the magnetic intensity of the magnetic rock packages. In general the shapes of the magnetic profiles are asymmetric. The shallow gradient corresponds to the shallowing of the tilt-block away from the half-graben bounding normal fault. The peak magnetic response is coincident with the tilt-block crest where the magnetic basement is at its shallowest level. The steep gradient in the magnetic profile is related to the offset of the magnetic basement across the normal faults. Shallow-dipping normal faults are characterised by a decrease in the magnetic gradient (cf. Fig. 10a and b).

Fig. 10c shows the same half-graben as that shown in Fig. 10a with 2-km-thick post-rift cover deposited on top. This situation is similar to many extensional basins that have been subject to post-rift thermal subsidence (e.g. McKenzie, 1978). In this model the shape of the magnetic profile is similar to other half-graben models, although the amplitude and the gradients of the magnetic response is decreased because the depth to the magnetic basement is greater. In the profiles shown in Fig. 10a–c, the peak magnetic response of the half-graben approximates the position of the normal fault.

Fig. 10d shows a simplified cross-section with a highly magnetic marker unit flooring the half-graben. As the susceptibility of the magnetic marker unit is four orders of magnitude greater than the surrounding rocks, the magnetic response reflects the vector addition of the three-dipping prisms that represent the magnetic marker unit. The other rock packages have very little influence on the magnetic response. The overall magnetic profile shape is similar to Fig. 10c, although the amplitudes of the magnetic anomalies are increased and the peak magnetic amplitude is located above the footwall of the normal faults, rather than at the tilt-block crest (Fig. 10d). The shift in peak magnetic response towards the footwall of the normal faults is caused because the affects of the dipping prism in the normal fault hanging wall is greater than in the other models. The asymmetry of the magnetic response, related to the shallowing of the magnetic marker unit along the tilt-block, is still evident.

In this model the highest magnetic signature is located at the edge of the basin, where the tilt-block has been eroded and the magnetic marker horizon is overlain by the thin post-rift signature. The relatively high amplitude of this anomaly reflects the shallow depth of the magnetic marker unit, resulting in a relatively sharp magnetic gradient compared with the half-graben.

4.2. Aeromagnetic response of inverted half-graben

A sequence of simplified inversion structures and their calculated aeromagnetic responses are presented in Fig. 11, using Fig. 10d as a starting geometry. This starting geometry was chosen because the magnetic stratigraphy is most like that of the Lawn Hill Platform in the Mount Isa Inlier. The continental tholeiitic basalts of the Eastern Creek Volcanics are the dominant influence on the magnetic signature throughout the Western Fold Belt ($1000–10000 \times 10^{-5}$ SI) (Leaman, 1991; Duffett, 1998; Betts, 1999). The thickness of the Eastern Creek Volcanics varies from 6–8 km in the Leichhardt River Fault Trough (Bain et al., 1992) to ~2 km in the southern Lawn Hill Platform

(Betts, 1997). The Eastern Creek Volcanics are locally demagnetised by alteration. A minor influence in the magnetic response includes the moderately magnetised ($1-100\times10^{-5}$ SI) syn-rift Fiery Creek Volcanics (Leaman, 1991; Betts, 1997; Duffett, 1998; Fig. 2). Sedimentary sequences belonging to the Leichhardt, Calvert and Isa superbasins are generally low- to non-magnetic (Betts, 1997; Duffett, 1998). Consequently, offset of pre-rift and syn-rift magnetic markers across the fault system should be delineated from aeromagnetic data.

Fig. 11a–c shows the magnetic response of simplified cross-sections of the progressive inversion of half-grabens and the associated development of isolated growth anticlines as the syn-rift units are expelled from the half-graben. In this scenario, inversion is achieved by reverse reactivation of the normal fault. Fig. 11d and e shows progressive inversion with buttressing of hanging wall successions against the footwall. In both scenarios complications such as development of break-back thrusts and movement along the pre-rift unconformity have not been modelled.

During reverse reactivation of the normal fault, expulsion of late syn-rift and post-rift stratigraphy occurs, resulting in reverse offset at the surface. The size of isolated growth anticlines increases as inversion increases (Fig. 11a and b). The magnetic response of this inversion geometry is influenced by the offset of the magnetic horizon beneath the half-graben. Preservation of normal offset of pre- and early-rift successions in the subsurface is reflected by the asymmetric magnetic profile typical of tilt-block rotation and half-graben with magnetic basement (Fig. 10).

However, the profile shape does change due to inversion (cf. Figs. 10d and 11a), and this is related to the decrease in the depth of the magnetic horizon. Fig. 11b and c shows the change in geometry associated with increased crustal shortening and inversion. Reverse offset at the surface is greater and there is a smaller component of normal offset of the pre-rift and early syn-rift successions in the subsurface. The magnetic profiles above the inverted half-graben display an asymmetric shape, although it is less pronounced, than the models shown in Figs. 10d and 11a. The peak magnetic response remains coincident with the location of the normal faults and the overall shape of the profile reflects the remnant half-graben geometry up until the stage where the half-graben have been completely inverted and there is reverse offset of the magnetic marker unit (Fig. 11c). At this stage the magnetic profile has lost its asymmetry and its shape is related to the depth and geometry to the pre-rift magnetic marker. The amplitudes and gradients in this magnetic profile are related to erosional truncations of the magnetic horizon, and the duplication of the magnetic marker horizon because of reverse reactivation.

Cross-sections showing hanging wall buttressing are presented in Fig. 11d and e. Buttressing of pre-, syn-, and post-rift successions has caused intense folding against the footwall buttress, and expulsion of syn- and post-rift successions out of the half-graben. In Fig. 11d inversion is relatively mild. The magnetic profile is complicated because of the folding of the pre-rift magnetic marker beds in the hanging wall; however, the asymmetry in the magnetic profile (typical of the half-graben models) is still evident because the pre-rift and early syn-rift successions preserve a component of normal offset in the subsurface, and the original half-graben geometry is partially preserved. The asymmetry is less pronounced because folding in the hanging wall brings the magnetic horizon closer to the surface. Magnetic amplitude peaks still coincide with the position of the normal fault. Fig. 11e shows intense buttressing with pre-rift successions in the subsurface having a small component of normal offset. The asymmetry in the magnetic profiles is due to intense hanging wall folding in which folded successions are brought closer to the surface. The transition from steep to shallow magnetic gradient in the hanging wall is coincident with the drop off in hanging wall strain, rather than where the normal fault and tilt-block intersect.

4.3. Lawn Hill Platform examples

Two examples of buried inverted half-graben are demonstrated in two-dimensional forward models of aeromagnetic data from the Lawn Hill Platform (Fig. 12b and c). The models assume that the thickness for the Eastern Creek Volcanics does not exceed 2.5 km (maximum thickness in the southern Lawn Hill Platform) and that the magnetic susceptibility is homogeneous (0.1 SI). The other rock types are modelled with the same low magnetic susceptibility (0–0.00001 SI). These constraints are consistent with measured magnetic susceptibility data from the southern Lawn Hill Platform (Betts, 1997). The models essentially show the sub-surface geometry of the highly magnetic basalts of the Eastern Creek Volcanics. The subsurface dips of the faults are unconstrained in the northern part of the Lawn Hill Platform. However, we inferred that the dips of the faults are similar to NW-dipping normal faults in the southern Lawn Hill Platform (Betts et al., 1999). The unconformity between the superbasins is interpretative and does not influence the magnetic signature of the Lawn Hill Platform. The profile locations are shown in Fig. 12a.

The central part of the cross-section (Fig. 12b) shows an asymmetric magnetic profile similar to the theoretical transects shown in Fig. 10a–d. This asymmetrical profile is modelled as a tilt-block crest bounded by a normal fault, which preserves 10 km offset of the Eastern Creek Volcanics in the subsurface (Fig. 12b). This offset represents the superimposed stratal-growth during the evolution of the Leichhardt and Calvert superbasins. The aeromagnetic response suggests the presence of a normal fault beneath the Ploughed Mountain and Mount Caroline anticlines (Fig. 12b). The Ploughed Mountain Anticline appears to have formed as a result of buttressing during inversion and its surface expression is interpreted as a result of folding against the buttress. This differs slightly from the

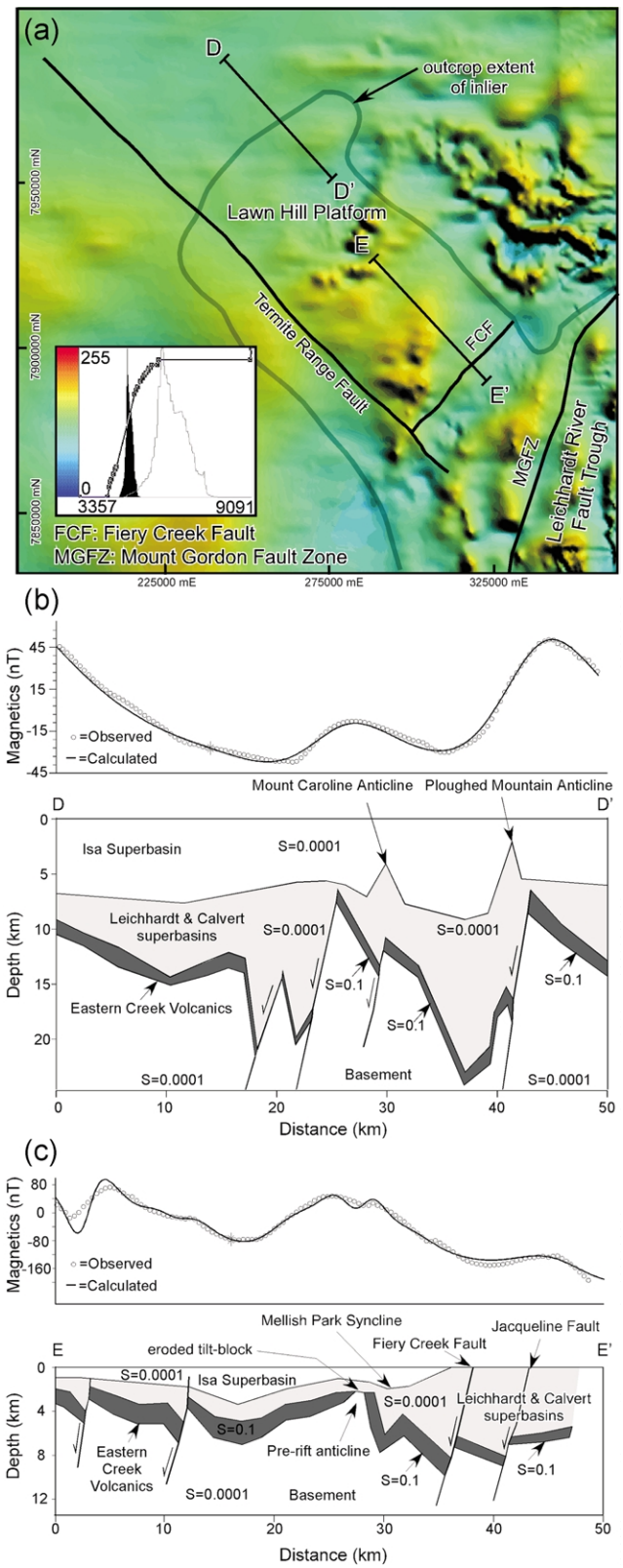

Fig. 12. (a) Reduced to the pole magnetic image of the Lawn Hill Platform. Image courtesy of Geoscience Australia. The position of the magnetic profiles depicted in (b) and (c) is shown. Image location is shown in Fig. 3. (b) Forward model of northern part of the exposed Lawn Hill Platform across the Ploughed Mountain and Mount Caroline anticlines. (c) Forward model of the magnetic profile across the Fiery Creek Fault system showing normal offset of the basement Eastern Creek Volcanics across the fault, and truncation of the Eastern Creek Volcanics by syn-MIRE unconformity on the tilt-block crest. The models shown in (b) and (c) represent the distribution of the magnetic Eastern Creek Volcanics. The other units have the same low magnetic susceptibilities and their boundaries (shown in dashed lines) are interpretative. The locations of major structures along the profiles are also shown.

growth anticline interpretation of Betts and Lister (2002) (see Fig. 9b). The model suggests that the fault preserves approximately 7 km normal offset, which occurred during the Leichhardt and Calvert superbasin phases (Fig. 12b). The model suggests that the Mount Caroline anticline is a growth anticline that developed above a smaller-scale normal fault within the larger half-graben, similar to that interpreted for the Moondarra Anticline in the Crystal Creek Block (Fig. 4a and b) (O'Dea and Lister, 1995).

The cross-section shown in Fig. 12c is located in the southern Lawn Hill Platform (Fig. 12a). The geometry of the Eastern Creek Volcanics has been influenced by the extensional evolution as well as a pre-Calvert Superbasin inversion event (Betts, 1999). This profile is also characterized by several asymmetric peaks and troughs that are modelled as a response to half-graben and eroded tilt-blocks of the folded Eastern Creek Volcanics. The profile transects the Jacqueline and Fiery Creek Fault systems (Fig. 3) and suggests they have a normal offset of several kilometres in the subsurface (Fig. 12b). The surface offset of the Fiery Creek Fault is variable from reverse to normal along its strike length (Betts, 2001). The model also suggests that there is a general thickening of the Leichhardt and Calvert Superbasin sediments to the southeast and that the Eastern Creek Volcanics are relatively shallow in the northern parts of the profile, despite being buried beneath successions of the Isa Superbasin. The symmetric shape of the profile in the central part of the cross-section is modelled as erosion of the Eastern Creek Volcanics along the western limb of the Mellish Park Syncline during the onset of the MIRE and is interpreted as a remnant tilt block crest. This is similar to the eroded tilt block in the theoretical models (Fig. 10c and d). The model also indicates the presence of several smaller normal faults in the northern part of the section.

5. Discussion

Many well-endowed basins that host SHMS Pb–Zn–Ag mineralization have been inverted during later orogenesis. Exploration for SHMS Pb–Zn–Ag relies on understanding the basin fault architecture as a vector for targeting potential conduits for mineralising fluids. Aeromagnetic datasets enable the interpretation of the three-dimensional geometry of structures in the subsurface and are therefore ideal tools for assessing basin architecture buried beneath younger cover, as well as subsurface offset of normal faults that have been reactivated during basin inversion. We have presented

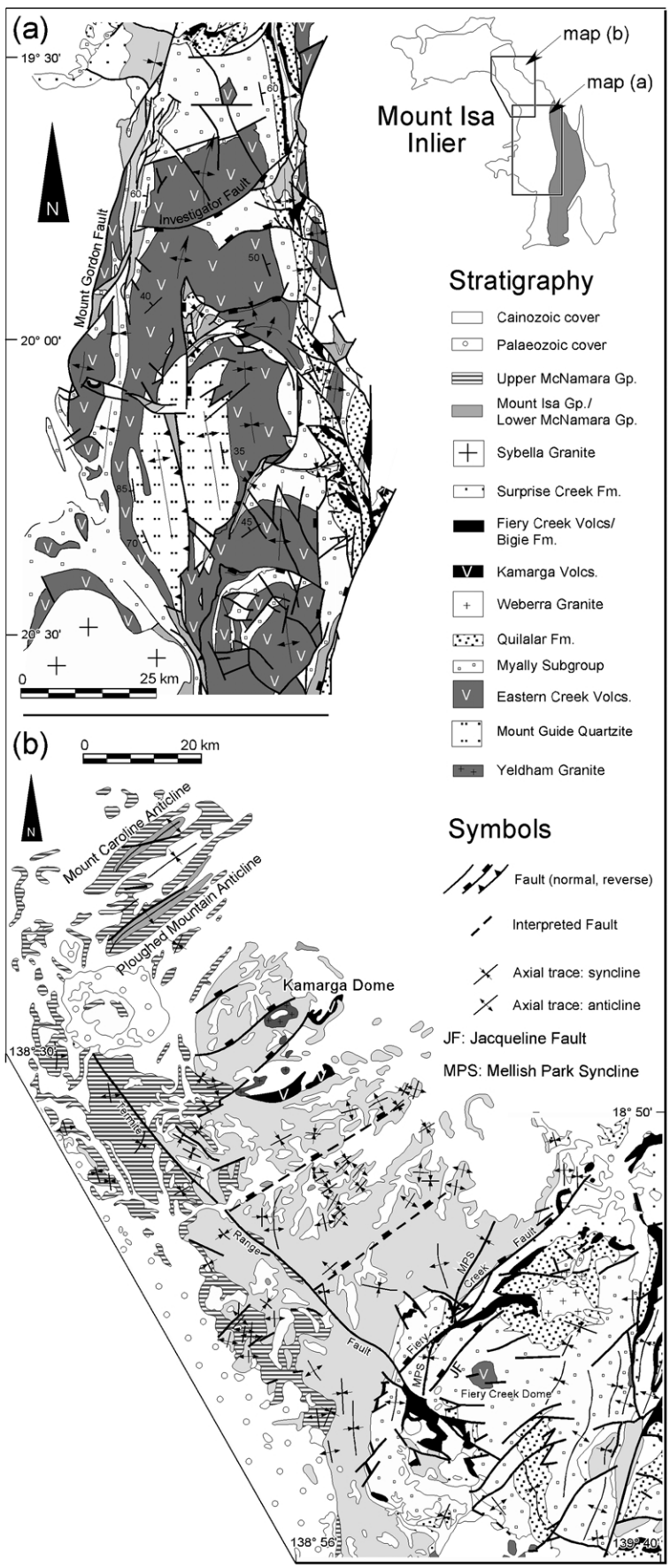
(a)
19° 30'
20° 00'
20° 30'
N
Mount Gordon Fault
Investigator Fault
0
25 km
map (b)
map (a)
Mount Isa Inlier
Stratigraphy
Cainozoic cover
Palaeozoic cover
Upper McNamara Gp.
Mount Isa Gp./ Lower McNamara Gp.
Sybella Granite
Surprise Creek Fm.
Fiery Creek Volcs/ Bigie Fm.
Kamarga Volcs.
Weberra Granite
Quilalar Fm.
Myally Subgroup
Eastern Creek Volcs.
Mount Guide Quartzite
Yeldham Granite
(b)
0
20 km
N
Mount Caroline Anticline
Ploughed Mountain Anticline
Kamarga Dome
Symbols
Fault (normal, reverse)
Interpreted Fault
Axial trace: syncline
Axial trace: anticline
JF: Jacqueline Fault
MPS: Mellish Park Syncline
138° 30'
18° 50'
Range
Fault
MPS
Creek
Fault
Fiery
MPS
JF
Fiery Creek Dome
138° 56'
139° 40'

an approach to assessing basin faults and inversion structures using integrated forward modelling of aeromagnetic data and conventional mapping techniques. Our approach involves modelling the magnetic responses of extensional and inversion structures, and then using these modelled forward magnetic responses to recognise basin structures. The approach is most effective if the structural framework has been determined from field mapping or seismic data and a magnetic stratigraphy has been established. This information reduces the ambiguity associated with developing forward models of potential field datasets.

In the magnetic forward models of half-graben and simplified inversion geometries, the location of the normal faults approximately coincided with the peak magnetic signature, and the tilt-block geometry was characterized by an asymmetric magnetic response. These relationships were relatively robust in models depicting mild inversion (0–25% shortening) because elements of the original half-graben geometry and normal subsurface offset were preserved. This approach is therefore most effective if: (1) inversion is relatively mild and elements of the basin architecture or half-graben structure are preserved; (2) there is a simplified magnetic stratigraphy or single magnetic marker horizon, which has been affected by the normal faulting (i.e. within lower syn-rift or pre-rift successions); and (3) the post-rift cover is non-magnetic and therefore does not mask the signature of the deeper extensional related structures.

The magnetic data could not be used to locate normal faults in models where hanging wall buttressing was intense or if there was complete inversion of the half-graben because either intense folding in the hanging wall obscures its magnetic signature or the normal component of offset of the magnetic marker units is not preserved. In these situations, basin faults may be recognised in regional map patterns as areas of intense local strain or as isolated anticlines in syn and post-rift succession. Recognition of normal faults in the subsurface using magnetic data becomes increasingly difficult if: (1) the magnetic stratigraphy is complicated and there are multiple magnetic horizons; and (2) there are no magnetic horizons in the stratigraphic pile. The effectiveness of the approach is limited if a geological framework cannot be determined to delineate geometrical constraints (e.g. dip direction) or a magnetic stratigraphy has not been defined.

Once a magnetic stratigraphy is established alternative magnetic responses for half-graben can be modelled. For example, if the syn-rift fill is magnetic and the pre-rift basement is non-magnetic then the magnetic response of the normal fault and half-graben will be markedly different. Fig. 11g shows the same geometry as the mildly inverted half-graben shown in Fig. 11a. However, in this model, syn-rift successions are magnetic and the basement is non-magnetic. The peak magnetic response is located where the syn-rift successions are thickest in the immediate hanging wall of the normal fault. The peak magnetic signature is therefore still coincident with the location of the normal fault. The steepest gradient is related to the thickness decrease of the syn-rift successions in the footwall of the fault and the shallowest gradient results from the gradual tapering of the half-graben wedge (Fig. 11g).

5.1. Regional considerations

The orientation and geometry of regional and local folds produced during the Isan Orogeny have been interpreted to reflect the regional shortening direction (e.g. Bell, 1983; Blake and Stewart, 1992). These interpretations have been challenged by the recognition of variable fold orientations and strain gradients in the hanging walls of extensional faults (O'Dea and Lister, 1995). Many fold orientations no longer can be interpreted to reflect the regional stress regime. In addition, there are marked differences, on a regional scale, in the orientation of faults active during the MIRE between the Leichhardt River Fault Trough and the Lawn Hill Platform (Betts et al., 1999).

The Leichhardt River Fault Trough is characterised by N- and E-oriented cross-rift normal faults (O'Dea et al., 1997b; Lister et al., 1999; Betts and Lister, 2001), whereas the Lawn Hill Platform is characterised by NE-trending normal faults and NW-striking transverse faults (Betts et al., 1999). These differences have been attributed to variations in the underlying pre-MIRE basin architecture (Betts et al., 1998, 1999). The N- and E-trending faults in the Leichhardt River Fault Trough appear to be controlled by structures formed during the evolution of the Leichhardt Superbasin, whereas the normal faults in the Lawn Hill Platform reflect the bulk strain associated with the MIRE. The axial traces of regional folds appear to mimic the orientation of extensional faults (Fig. 13a and b). In the Leichhardt River Fault Trough the regional fold pattern is characterised by folds with E–W and N–S axial traces. There is spatial correlation between the location of E–W oriented folds and E-trending cross-rift structures (see O'Dea et al. (1997b)) (Fig. 13a). E–W oriented folds are not preserved away from cross-rift faults (Lister et al., 1999; Fig. 5). The dominant regional N–S, upright, shallowly to moderately plunging folds in the Leichhardt River Fault Trough are parallel to the original

Fig. 13. (a) Regional map of the Leichhardt River Fault Trough showing the location and orientation of major extensional faults. These faults have dominantly N–S and E–W orientations and have been active throughout the evolution of the Leichhardt, Calvert and Isa Superbasins (adapted after O'Dea et al., 1997b). (b) Regional map of the Lawn Hill Platform showing the orientations of extensional faults and major folds. (a) and (b) Show that the orientation of the axial traces of regional folds is parallel to the extensional fault architecture, and the variations in the fault pattern result in variations in the regional fold pattern.

orientation of the rift axis, and developed during the second phase of basin inversion (O'Dea et al., 1997a,b) (Fig. 13b).

Regional folds in the relatively mildly deformed Lawn Hill Platform are dominated by upright to doubly plunging folds with NE-oriented axial traces that are parallel to the normal faults throughout the platform (Fig. 13b). The Mount Caroline and Ploughed Mountain anticlines appear to have formed as a direct consequence of half-graben inversion during the Isan Orogeny. We suggest that the differences in the trend of axial traces between the Lawn Hill Platform and the Leichhardt River Fault Trough reflects the influence of the underlying extensional fault architecture rather than a change in the regional stress regime.

6. Conclusion

Integrated structural and aeromagnetic analyses are effective tools for mapping extensional faults and half-graben in partially inverted and buried basins. Ancient inverted normal faults may be located by anomalously high hanging wall strain related to buttressing against a rigid footwall, the development of isolated growth anticlines, and enigmatic fold orientations, which are inconsistent with inferred regional shortening directions. The aeromagnetic response of half-graben with a magnetic basement is characterized by an asymmetric magnetic profile. Shallow gradients are related to shallowing of the tilt-block and steep gradients in the profile are related to normal offset and deepening of the magnetic basement. The peak in the magnetic profile is approximately coincident with the location of the normal fault. The asymmetric shape of the profile is maintained during the formation of inversion-related growth anticlines and mild buttressing. The location of the normal faults also remains coincident with the peak magnetic response of the half-graben during mild inversion. The effectiveness of aeromagnetic analysis for mapping buried or obscured half-graben is lost after intense inversion. Reverse reactivation of the magnetic basement and the intense hanging wall buttressing alters the magnetic profiles such that the original asymmetry of the half-graben is either lost or no longer represents the half-graben geometry.

Acknowledgements

We would like to thank Caroline Forbes for drafting several figures and Matt Betts, Lisa O'Neill, and Jane Richardson for their assistance in the field. The research was funded in part from an ARC SPIRT grant with WMC Resources and the Australian Geodynamics Cooperative Research Centre. The aeromagnetic image published in Fig. 12a is published with permission of the Executive Director of Geoscience Australia. We thank Bruce Goleby and Klaus Gessner for their thorough reviews, which improved the paper.

References

Andrews, S.J., 1998. Stratigraphy and depositional setting of the upper McNamara Group, Lawn Hills region, Northwest Queensland. Economic Geology 93, 1132–1152.

Badley, M.E., Price, J.D., Backshall, L.C., 1989. Inversion, reactivated faults and related structures: seismic examples from the southern North Sea. In: Cooper, M.A., Williams, G.D. (Eds.), Inversion Tectonics. Special Publication of the Geological Society of London 44, 201–219.

Bain, J.H.C., Heinrich, C.A., Henderson, G.A.M., 1992. Stratigraphy, structure and metasomatism of the Haslingden Group, East Moondarra area, Mount Isa: a deformed and mineralised Proterozoic multi-stage rift-sag sequence. Australian Geological Survey Organisation Bulletin 243, 125–136.

Bell, T.H., 1983. Thrusting and duplex formation at Mt Isa, Queensland, Australia. Nature 304, 493–497.

Betts, P.G., 1997. The Mount Isa Rift Event: a Middle Proterozoic example of intracontinental extension. PhD Thesis, Monash University, Melbourne, Victoria.

Betts, P.G., 1999. Palaeoproterozoic mid-basin inversion in the northern Mt Isa terrane, Queensland. Australian Journal of Earth Sciences 46, 735–748.

Betts, P.G., 2001. Three-dimensional structure along the inverted Palaeoproterozoic Fiery Creek Fault system, Mount Isa terrane, Australia. Journal of Structural Geology 23, 1953–1969.

Betts, P.G., Lister, G.S., 2001. A comparison of the "strike-slip" versus the "episodic rift-sag" models for the origin of the Isa Superbasin. Australian Journal of Earth Sciences 48, 265–280.

Betts, P.G., Lister, G.S., 2002. Geodynamically indicated targeting strategy for shale hosted massive sulphide Pb–Zn mineralisation in the Western Fold Belt of the Mount Isa terrane. Australian Journal of Earth Sciences 49, 985–1010.

Betts, P.G., Lister, G.S., O'Dea, M.G., 1998. Asymmetric extension of the Middle Proterozoic lithosphere, Mount Isa terrane, Queensland, Australia. Tectonophysics 296, 293–316.

Betts, P.G., Lister, G.S., Pound, K.S., 1999. Architecture of a Palaeoproterozoic rift system; evidence from the Fiery Creek Dome region, Mt. Isa terrane. Australian Journal of Earth Sciences 46, 533–554.

Betts, P.G., Lister, G.S., Giles, D., 2003. Tectonic environment of shale-hosted massive sulfide Pb–Zn–Ag deposits of Proterozoic northeastern Australia. Economic Geology 98, 557–576.

Blake, D.H., 1987. Geology of the Mount Isa Inlier and environs, Queensland and Northern Territory. BMR Bulletin 225, 83.

Blake, D.H., Stewart, A.J., 1992. Stratigraphic and tectonic framework, Mount Isa Inlier. Australian Geological Survey Organisation Bulletin 243, 1–11.

Broadbent, G.C., Myers, R.E., Wright, J.V., 1998. Geology and origin of shale-hosted Zn–Pb–Ag mineralization at the Century Deposit, Northwest Queensland, Australia. Economic Geology 93, 1264–1294.

Bull, S.W., Rogers, J.R., 1996. Recognition and significance of an early compressional deformational event in the Tawallah Group, McArthur Basin, NT. James Cook University of North Queensland Research Unit Contribution 55, 28–32.

Butler, R.W.H., 1989. The influence of pre-existing basin structure on thrust system evolution in the Western Alps. In: Cooper, M.A., Williams, G.D. (Eds.), Inversion Tectonics. Special Publication of the Geological Society of London 44, 17–39.

Carr, G.R., 1996. Recent developments in the use of Pb-isotope models in Proterozoic terranes. James Cook University of North Queensland Research Unit Contribution 55, 33–35.

Cox, S.F., Knackstedt, M.A., Braun, J., 2001. Principles of structural

control on permeability and fluid flow in hydrothermal systems. Reviews in Economic Geology 14, 1–24.

Derrick, G.M., 1982. A Proterozoic rift zone at Mount Isa, Queensland, and implications for mineralisation. BMR Journal of Australian Geology and Geophysics 7, 81–92.

Derrick, G.M., 1996. The "geophysical" approach to metallogeny of the Mt. Isa Inlier; what sort of orebody do you want? Australasian Institute of Mining and Metallurgy Publication Series 1/96, 349–366.

Derrick, G.M., Sweet, I.P., Hutton, L., Wilson, I.H., Perkins, W., 1983. Geology of the Mount Oxide Region. Australia 1:100,000 geological special. Bureau of Mineral Resources, scale, 1:100,000, 1 sheet.

Duffett, M.L., 1998. Gravity, magnetic and radiometric evidence for the geological setting of the Lady Loretta Pb–Zn–Ag deposit—a qualitative appraisal. Economic Geology 93, 1295–1306.

Eriksson, K.A., Simpson, E.L., Jackson, M.J., 1993. Stratigraphical evolution of a Proterozoic syn-rift to post-rift basin: constraints on nature of lithospheric extension in the Mount Isa Inlier, Australia. Special Publication of the International Association of Sedimentologists 20, 203–221.

Etheridge, M.A., 1986. On the reactivation of the extensional fault system. Philosophical Transactions of the Royal Society of London Series A: Mathematical and Physical Sciences 317, 179–194.

Etheridge, M.A., Wall, V.J., 1994. Tectonic and structural evolution of the Australian Proterozoic. Geological Society of Australia Abstracts 37, 102–103.

Garven, G., Bull, S.W., Large, R.R., 2001. Hydrothermal fluid flow models of stratiform ore genesis in the McArthur Basin, Northern Territory, Australia. Geofluids 1, 289–311.

Giles, D., Betts, P.G., Lister, G.S., 2002. A continental back-arc setting for early to Middle Proterozoic basins of northeastern Australia. Geology 30, 823–826.

Goodfellow, W.D., Lydon, J.W., Turner, R.J.W., 1993. Geology and genesis of stratiform sediment-hosted (SEDEX) zinc–lead–silver sulphide deposits. Geological Association of Canada Special Paper 40, 201–251.

Grant, F.S., 1984a. Aeromagnetics, geology and ore environments, I. Magnetite in igneous rocks, sedimentary and metamorphic rocks: an overview. Geoexploration 23, 303–333.

Grant, F.S., 1984b. Aeromagnetics, geology and ore environments, II. Magnetite and ore environments. Geoexploration 23, 335–362.

Gunn, P.J., Maidment, D., Milligan, P.R., 1997. Interpreting aeromagnetic data in areas of limited outcrop. AGSO Journal of Australian Geology and Geophysics 17, 175–186.

Gustafson, L.B., Williams, N., 1981. Sediment-hosted stratiform deposits of copper, lead, and zinc. Economic Geology 75, 139–178.

Hayward, A.B., Graham, R.H., 1989. Some geometrical characteristics of inversion. In: Cooper, M.A., Williams, G.D. (Eds.), Inversion Tectonics. Special Publication of the Geological Society of London 44, 17–39.

Hill, K.C., Hill, K.A., Cooper, G.T., O'Sullivan, A.J., O'Sullivan, P.B., Richardson, M.J., 1995. Inversion around the Bass Basin, SE Australia. In: Buchanan, J.G., Buchanan, P.G. (Eds.), Basin Inversion. Special Publication of the Geological Society of London 88, 525–548.

Hobbs, B.E., Ord, A., Archibald, N.J., Walshe, J.L., Zhang, Y., Brown, M., Zhao, C., 2000. Geodynamic modelling as an exploration tool. Australian Institute of Mining and Metallurgy Publication Series 2/2000, 34–49.

Hornby, P., Boschetti, F., Horowitz, F.G., 1999. Analysis of potential field data in the wavelet domain. Geophysical Journal International 137, 175–196.

Jackson, M.J., Scott, D.L., Rawlings, D.J., 2000. Stratigraphic framework for the Leichhardt and Calvert Superbasins: review and correlations of the pre-1700 Ma successions between Mt Isa and McArthur River. Australian Journal of Earth Sciences 47, 381–404.

Jessell, M.W., Valenta, R.K., Jung, G., Geiro, A., 1993. Structural geophysics. Exploration Geophysics 24, 599–602.

Kelly, P.G., Peacock, D.C.P., Sanderson, D.J., McGurk, A.C., 1999. Selective reverse-reactivation of normal fault, and deformation around reverse-reactivation faults in the Mesozoic of the Somerset coast. Journal of Structural Geology 21, 493–509.

Leaman, D.E., 1991. Geophysical constraints on structure and alteration of the Eastern Creek Volcanics, Mt. Isa, Queensland. Australian Journal of Earth Sciences 38, 457–472.

Lillie, R.J., 1998. Whole Earth Geophysics: An Introductory Textbook for Geologists and Geophysicists. Prentice Hall, New Jersey, 361pp.

Lister, G.S., O'Dea, M.G., Somaia, I., 1999. A tale of two synclines: rifting, inversion and transpressional popouts at Lake Julius, northwestern Mount Isa terrane, Queensland. Australian Journal of Earth Sciences 46, 233–250.

Lowell, J.D., 1995. Mechanics of basin inversion from world-wide examples. In: Buchanan, J.G., Buchanan, P.G. (Eds.), Basin Inversion. Special Publication of the Geological Society of London 88, 39–57.

McClay, K.R., 1989. Analogue models of inversion tectonics. In: Cooper, M.A., Williams, G.D. (Eds.), Inversion Tectonics. Special Publication of the Geological Society of London 44, 41–59.

McClay, K.R., 1995. The geometry and kinematics of inverted fault systems: a review of analogue model studies. In: Buchanan, J.G., Buchanan, P.G. (Eds.), Basin Inversion. Special Publication of the Geological Society of London 88, 97–118.

McGoldrick, P.J., Large, R., 1998. Proterozoic stratiform sediment-hosted Zn–Pb–Ag deposits. Australian Geological Survey Organisation Journal of Geology and Geophysics 17, 189–196.

MacGregor, D.S., 1995. Hydrocarbon habitat and classification of inverted rift basins. In: Buchanan, J.G., Buchanan, P.G. (Eds.), Basin Inversion. Special Publication of the Geological Society of London 88, 83–93.

McKenzie, D., 1978. Some remarks on the development of sedimentary basins. Earth and Planetary Science Letters 40, 25–32.

Myers, J.S., Shaw, R.D., Tyler, I.M., 1996. Tectonic evolution of Proterozoic Australia. Tectonics 15, 1431–1446.

Nelson, J., Paradis, S., Christensen, J., Gabites, J., 2002. Canadian Cordillera Mississippi Valley-type deposits: a case for Devonian–Mississippian back-arc hydrothermal origin. Economic Geology 97, 1013–1036.

Neudert, M.K., McGeough, M., 1996. A new tectonostratigraphic framework for the deposition of the upper McArthur Group, NT. James Cook University of North Queensland Economic Geology Research Unit, Extended Abstracts 55, 90–94.

Nijman, W., van Lochem, J.H., Spliethoff, H., Feijth, J., 1992. Deformation model and sedimentation patterns of the Proterozoic of the Paroo Range, Mount Isa Inlier, Queensland, Australia. AGSO Bulletin 243, 29–73.

O'Dea, M.G., 1996. Geometry and structural evolution of the Leichhardt River Fault Trough, Mount Isa terrain, Australia. PhD Thesis, Monash University, Melbourne, Victoria.

O'Dea, M.G., Lister, G.S., 1995. The role of ductility contrast and basement architecture in the structural evolution of the Crystal Creek Block, Mount Isa Inlier, Australia. Journal of Structural Geology 17, 949–960.

O'Dea, M.G., Lister, G.S., MacCready, T., Betts, P.G., Oliver, N.H.S., Pound, K.S., Huang, W., Valenta, R.K., 1997a. Geodynamic evolution of the Proterozoic Mount Isa terrain. In: Burg, J.-P., Ford, M. (eds.) Geological Society of London Special Publication 121, 99–122.

O'Dea, M.G., Lister, G.S., Betts, P.G., Pound, K.S., 1997b. A shortened intraplate rift system in the Proterozoic Mount Isa terrain, NW Queensland, Australia. Tectonics 16, 425–441.

Ord, A., Hobbs, B.E., Zhang, Y., Broadbent, G.C., Brown, M., Willets, G., Sorjonen-Ward, P., Walshe, J.L., Zhao, C., 2002. Geodynamic modelling of the Century deposit, Mount Isa Province, Queensland. Australian Journal of Earth Sciences 49, 1011–1039.

Page, R.W., Sun, S.S., 1998. Aspects of geochronology and crustal evolution in the Eastern Fold Belt, Mt Isa Inlier. Australian Journal of Earth Sciences 45, 343–361.

Page, R.W., Sweet, I.H., 1998. Geochronology of basin phases in the western Mount Isa Inlier, and correlation with the McArthur Basin. Australian Journal of Earth Sciences 45, 219–232.

Page, R.W., Sun, S.S., MacCready, T., 1997. New geochronological results in the central and eastern Mount Isa Inlier and implications for mineral exploration. Geodynamics and Ore Deposits Conference, Australian Geodynamics Cooperative Research Centre Abstracts, pp. 46–48.

Page, R.W., Jackson, M.J., Krassay, A.A., 2000. Constraining sequence stratigraphy in north Australian basins: SHRIMP U–Pb zircon geochronology between Mt Isa and McArthur River. Australian Journal of Earth Sciences 47, 431–460.

Plumb, K.A., Ahmad, M., Wygralak, A.S., 1990. Mid-Proterozoic basins of the North Australian Craton; regional geology and mineralisation. In: Hughes, F.E. (Ed.), Geology of the Mineral Deposits of Australia and Papua New Guinea. Australasian Institute of Mining and Metallurgy Monograph 14, pp. 881–902.

Rawlings, D.J., 1999. Stratigraphic resolution of a multiphase intracratonic basin system: the McArthur Basin, northern Australia. Australian Journal of Earth Sciences 46, 703–723.

Roberts, D.G., 1989. Basin inversion in and around the British Isles. In: Cooper, M.A., Williams, G.D. (Eds.), Inversion Tectonics. Special Publication of the Geological Society of London 44, 131–150.

Scott, D.L., Bradshaw, B.E., Tarlowski, C.Z., 1998. The tectonostratigraphic history of the Proterozoic northern Lawn Hill Platform, Australia: an integrated intracontinental basin analysis. Tectonophysics 300, 329–358.

Scott, D.L., Rawlings, D.J., Page, R.W., Tarlowski, C.Z., Idnurm, M., Jackson, M.J., Southgate, P.N., 2000. Basement framework and geodynamic evolution of the Palaeoproterozoic superbasins of north central Australia: an integrated review of geochemical, geochronological and geophysical data. Australian Journal of Earth Sciences 47, 341–380.

Selley, D., Winefield, P., Bull, S.W., Scott, R.J., McGoldrick, P.J., 2001. Sub-basins, depositional and tectonosedimentary setting of the HYC Zn–Pb–Ag deposit. Geological Society of America Abstacts 33, A-270.

Sibson, R.H., 1995. Selective fault reactivation during basin inversion; potential for fluid redistribution through fault-valve action. In: Buchanan, J.G., Buchanan, P.G. (Eds.), Basin Inversion. Special Publication of the Geological Society of London 88, 3–19.

Sibson, R.H., Moore, J.M., Rankin, A.H., 1975. Seismic pumping; a hydrothermal fluid transport mechanism. Journal of the Geological Society of London 131, 653–659.

Southgate, P.N., Bradshaw, B.E., Domagala, J., Jackson, M.J., Idnurm, M., Krassay, A.A., Page, R.W., Sami, T.T., Scott, D.L., Lindsay, J.F., McConachie, B.M., Tarlowski, C., 2000a. Chronostratigraphic basin framework for Palaeoproterozoic rocks (1730–1575 Ma) in northern Australia and implications for base-metal mineralisation. Australian Journal of Earth Sciences 47, 461–484.

Southgate, P.N., Scott, D.L., Sami, T.T., Domagala, J., Jackson, M.J., James, N.P., Kyser, T.K., 2000b. Basin shape and sediment architecture in the Gun Supersequence: a strike-slip model for Pb–Zn–Ag ore genesis at Mt Isa. Australian Journal of Earth Sciences 47, 509–532.

Valenta, R.K., Jessell, M.W., Jung, G., Bartlett, J., 1992. Geophysical interpretation and modelling of three-dimensional structure in the Duchess area, Mount Isa Inlier, Australia. Exploration Geophysics 23, 393–400.

Whiting, T.H., 1986. Aeromagnetics as an aid to geological mapping—a case history from the Arunta Inlier, Northern Territory. Australian Journal of Earth Sciences 33, 271–286.

Williams, G.G., Powell, C.M., Cooper, M.A., 1989. Geometry and kinematics of inversion tectonics. In: Cooper, M.A., Williams, G.D. (Eds.), Inversion Tectonics. Special Publication of the Geological Society of London 44, 3–15.